Biochemical and Biophysical Research Communications 450 (2014) 1505–1511

Contents lists available at ScienceDirect

Biochemical and Biophysical Research Communications

journal homepage: www.elsevier.com/locate/ybbrc

Autophagy is induced by raptor degradation via the ubiquitin/proteasome system in granular corneal dystrophy type 2

Seung-il Choi [a], Yong-Sun Maeng [a], Kyu Seo Kim [b], Tae-im Kim [a], Eung Kweon Kim [a,c,*]

[a] Cornea Dystrophy Research Institute and Department of Ophthalmology, Yonsei University College of Medicine, Seoul, Republic of Korea
[b] School of Medicine, Emory University, Atlanta, GA, United States
[c] BK21 Project for Medical Science and Severance Biomedical Science Institute, Yonsei University College of Medicine, Republic of Korea

ARTICLE INFO

Article history:
Received 2 July 2014
Available online 17 July 2014

Keywords:
Autophagy
Granular corneal dystrophy type 2
mTOR
Raptor
TGFBIp
Ubiquitin/proteasome system

ABSTRACT

Granular corneal dystrophy type 2 (GCD2) is an autosomal dominant disorder that is caused by a point mutation in transforming growth factor-β-induced gene-h3 (*TGFBI*), which encodes transforming growth factor-β-induced protein (TGFBIp). Recently, we found that the autophagic clearance of mutant-TGFBIp is delayed in GCD2 corneal fibroblasts; however, any potential correlation between mutant-TGFBIp turnover and autophagy–lysosome pathway remains unknown. Here, we report that mutant-TGFBIp is accumulated and that autophagy, a key clearance pathway for mutant-TGFBIp, is induced in primary cultured GCD2 homozygous (HO) and wild-type (WT) corneal fibroblasts that express exogenously introduced mutant-TGFBIp. Mutant-TGFBI colocalized with LC3-enriched cytosolic vesicles and cathepsin D in primary cultured GCD2 corneal fibroblasts. We also observed reduced levels of raptor (regulatory-associated protein of the mammalian target of rapamycin [mTOR]) in GCD2 corneal fibroblasts and WT corneal fibroblasts expressing mutant-TGFBIp. Strikingly, treatment with MG132, a ubiquitin/proteasome system inhibitor, significantly increased the levels of both total and ubiquitinated raptor in GCD2 corneal fibroblasts. The levels of the autophagy marker LC3-II were also increased in WT corneal fibroblasts that were treated with shRNA against raptor. However, mutant-TGFBIp accumulated in autophagosomes or/and lysosomes in spite of the significant activation of basal autophagy in GCD2 corneal fibroblasts. These results suggest that an insufficient autophagy–lysosome pathway might be responsible for the intracellular accumulation of mutant-TGFBIp during the pathogenesis of GCD2.

1. Introduction

All cells have surveillance systems that regulate the quality of proteins and organelles and eliminate any misfolded, malfunctioning, or damaged intracellular components [1,2]. Two important proteolytic systems remove abnormal proteins: the ubiquitin/proteasome system (UPS) and the autophagy–lysosome pathway [1]. Although the UPS and autophagy were thought to be independent degradation pathways, it was recently reported that ubiquitination could target substrates for degradation via both pathways. Moreover, impairment of the UPS is compensated for by the upregulation of autophagy [3].

Autophagy involves the sequestration of macromolecules and organelles into specialized cytosolic vesicles for their subsequent degradation in lysosomes [4,5]. It is activated when cells are exposed to various stresses such as starvation, the accumulation of damaged organelles, or oxidative stress [6]. Autophagy is tightly regulated by several signaling pathways, the best-characterized of which is the mTOR pathway. mTOR is a multi-domain protein kinase that interacts with other proteins to form two main complexes: mTORC1 and mTORC2. mTORC1 is composed of mTOR, G-protein β-subunit like protein (GβL), and regulatory associated protein of mTOR (raptor), and it is sensitive to rapamycin [7]. The rapamycin-insensitive complex mTORC2 is composed of mTOR, GβL, rapamycin-insensitive companion of mTOR (rictor), stress-activated-protein-kinase-interacting protein 1 (SIN1), and protein observed with rictor (protor) [7,8]. mTORC1 regulates protein synthesis and nutrient import, and it is a negative regulator of autophagy that senses signals through an upstream signaling cascade via class 1 phosphatidylinositol-3 kinase [5,9,10]. The inhibition of mTORC1 is sufficient to induce autophagy, suggesting that it serves as the major gatekeeper of autophagy induction in unstressed conditions [11,12].

* Corresponding author at: Department of Ophthalmology, Yonsei University College of Medicine, 50 Yonsei-ro, Seodaemun-gu, Seoul 120-752, Republic of Korea. Fax: +82 02 312 0541.
E-mail address: eungkkim@yuhs.ac (E.K. Kim).

http://dx.doi.org/10.1016/j.bbrc.2014.07.035
0006-291X/

Granular corneal dystrophy type 2 (GCD2, also called Avellino corneal dystrophy) is an autosomal-dominant disorder caused by a point mutation (R124H) in the *TGFBI* gene on chromosome 5q31 [13]. The age-dependent progressive accumulation of hyaline and amyloid in the corneal stroma is a hallmark of GCD2, and this results in the interference of corneal transparency [13–15].

We previously demonstrated the occurrence of oxidative stress [16] and altered mitochondrial function [17] in primary cultured GCD2 corneal fibroblasts. We also showed the delayed degradation of mutant-TGFBIp by the autophagy–lysosome system and elevated levels of ubiquitinated proteins in GCD2 corneal fibroblasts [18]. However, the mechanisms that stimulate autophagic activity in GCD2 corneal fibroblasts that accumulate TGFBIp are unknown. Because autophagy is induced by various stresses including the accumulation of damaged organelles and proteins, and oxidative stress [6], we hypothesized that accumulated mutant-TGFBIp is a proximal trigger of autophagy in GCD2.

2. Materials and methods

2.1. Materials

The proteasomal inhibitor MG132 and the lysosomal inhibitors bafilomycin A1, leupeptin, rapamycin, cycloheximide, dimethylsulfoxide, and 3-MA were obtained from Sigma (St. Louis, MO). SuperSignal West Pico chemiluminescent substrate was obtained from Pierce (Pierce, Rockford, IL). Anti-TGFBIp (R&D Systems, Minneapolis, MN), anti-β-actin (Sigma), anti-LC3, anti-p70S6K, anti-p-p70S6K, and anti-beclin-1 antibodies (Cell Signaling Technology, Beverly, MA), and an mTOR pathway antibody sampler kit (Cell Signaling Technology) were used as the primary antibodies. Horseradish peroxidase-linked anti-mouse or anti-rabbit IgG were used as secondary antibodies (Amersham Pharmacia Biotechnology, Piscataway, NJ).

2.2. Isolation and culture of primary corneal fibroblasts

Wild-type (WT) ($n = 3$), heterozygous (HT) ($n = 3$), and homozygous (HO) ($n = 3$) primary corneal fibroblasts were prepared as described previously [16]. The age, gender, and diagnosis of all GCD2 patients from which the cells were generated are listed in Table 1 of reference #18 [18]. Donor confidentiality was maintained in accordance with the Declaration of Helsinki, and the study was approved by the Severance Hospital IRB Committee (CR04124), Yonsei University, Seoul, Korea. GCD2 was diagnosed by DNA sequence analysis for *TGFBI* gene mutations.

2.3. Cell treatment and serum starvation

Bafilomycin A1, which inhibits autophagy by blocking the vacuolar adenosine triphosphate pump, was used at a concentration of 100 nM. Leupeptin (5–10 μg/ml), which inhibits cathepsins, was dissolved in dimethylsulfoxide (DMSO). Rapamycin was dissolved in DMSO immediately before use, and was added to the culture medium at concentrations of 100–200 nM. For serum starvation, cells were washed twice with phosphate-buffered saline (Gibco, Life Technologies, Grand Island, NY) and incubated in serum-free Dulbecco's modified Eagle's medium (Gibco, Life Technologies) at 37 °C for 3 h.

2.4. Preparation of cell lysates, Western blotting, immunoprecipitation, and real-time PCR

Cell lysates were prepared from primary cultured corneal fibroblasts in radioimmunoprecipitation assay buffer (150 mM NaCl, 1% NP-40, 0.5% deoxycholate, 0.1% sodium dodecyl sulfate [SDS], 50 mM Tris–HCl, pH 7.4) containing a protease inhibitor tablet (Complete Mini Protease Inhibitor Tablet, Roche). Crude cell lysate preparations and Western blotting were performed as described previously [16]. Co-immunoprecipitation using magnetic beads coated with polyclonal anti-raptor antibodies (3 μg/mL lysate; Bethyl Laboratories, Montgomery, TX, USA) was performed following the manufacturer's instructions (Invitrogen Dynal AS, Oslo, Norway). The immunoprecipitated proteins were then separated on 7.5% Tris/glycine SDS polyacrylamide gels. The intensities and optical densities of scanned immunoreactive protein bands were quantified using computer software (ImageJ, version 1.37, Wayne Rasband, NIH, USA), and corrected by background subtraction and normalization to the intensity of β-actin bands. Real-time PCR was performed as described previously [19].

2.5. Immunocytochemical staining

Immunofluorescence was performed as previously described [18]. Cells were viewed under a Leica TCS SP5 confocal microscope (Leica, Microsystems CMS GmbH, Germany). The following primary antibodies were used: monoclonal anti-TGFBIp (kindly provided by Dr. IS, Kim, Kyungpook National University, Korea), polyclonal anti-TGN 46 (Abcam, Cambridge, MA), anti-cathepsin-D rabbit polyclonal (Calbiochem, La Jolla, CA), and anti-LC3 (Cell Signaling Technology). Alexa 594 (red)-conjugated anti-rabbit (Vector Laboratories Inc., Burlingame, CA) and fluorescein isothiocyanate (green)-labeled anti-mouse IgG (Jackson ImmunoResearch Laboratories, West Grove, PA) secondary antibodies were used.

2.6. Adenoviral vectors

Adenoviruses expressing green fluorescent protein (GFP), or WT- and mutant-TGFBIp were generated using the AdEasy system [20]. Infection was performed as described previously [16].

2.7. Statistical analysis

The results were evaluated for statistical significance ($P < 0.05$) by using one-way analysis of variance (ANOVA) followed by Newman–Keuls multiple comparison tests. Results are expressed as means ± SDs. All data were processed using Graph Pad Prism software version 4.0 (Graph Pad Software Inc., San Diego, CA).

3. Results

3.1. Decreased TGFBI mRNA expression, and oligomerized and accumulated mutant-TGFBIp in GCD2 corneal fibroblasts

Because the degradation of mutant-TGFBIp is incomplete in GCD2 cells [18], we compared the levels of TGFBI mRNA and protein between three WT and GCD2 cells (three HO and one HT) by using real-time PCR and Western blotting, respectively, to identify whether mutant-TGFBIp accumulated in GCD2 cells. Varying amounts of TGFBIp were produced among samples (Fig. 1A). Although the protein abundance was comparable between WT and HO (Fig. 1B), the mRNA abundance was significantly lower (29.63 ± 10.69%, $P < 0.05$) in HO compared with WT cells (Fig. 1C). We next evaluated the ratio of TGFBI protein/mRNA. ANOVA revealed that the ratio was increased significantly (346.9 ± 282.5%, $P < 0.05$) in GCD2 cells compared with WT corneal fibroblasts (Fig. 1D). These results suggest that the accumulation of mutant-TGFBIp in GCD2 corneal fibroblasts might be due to defective degradation. To confirm this, we investigated the localization of intracellular TGFBIp using immunofluorescence. WT and GCD2

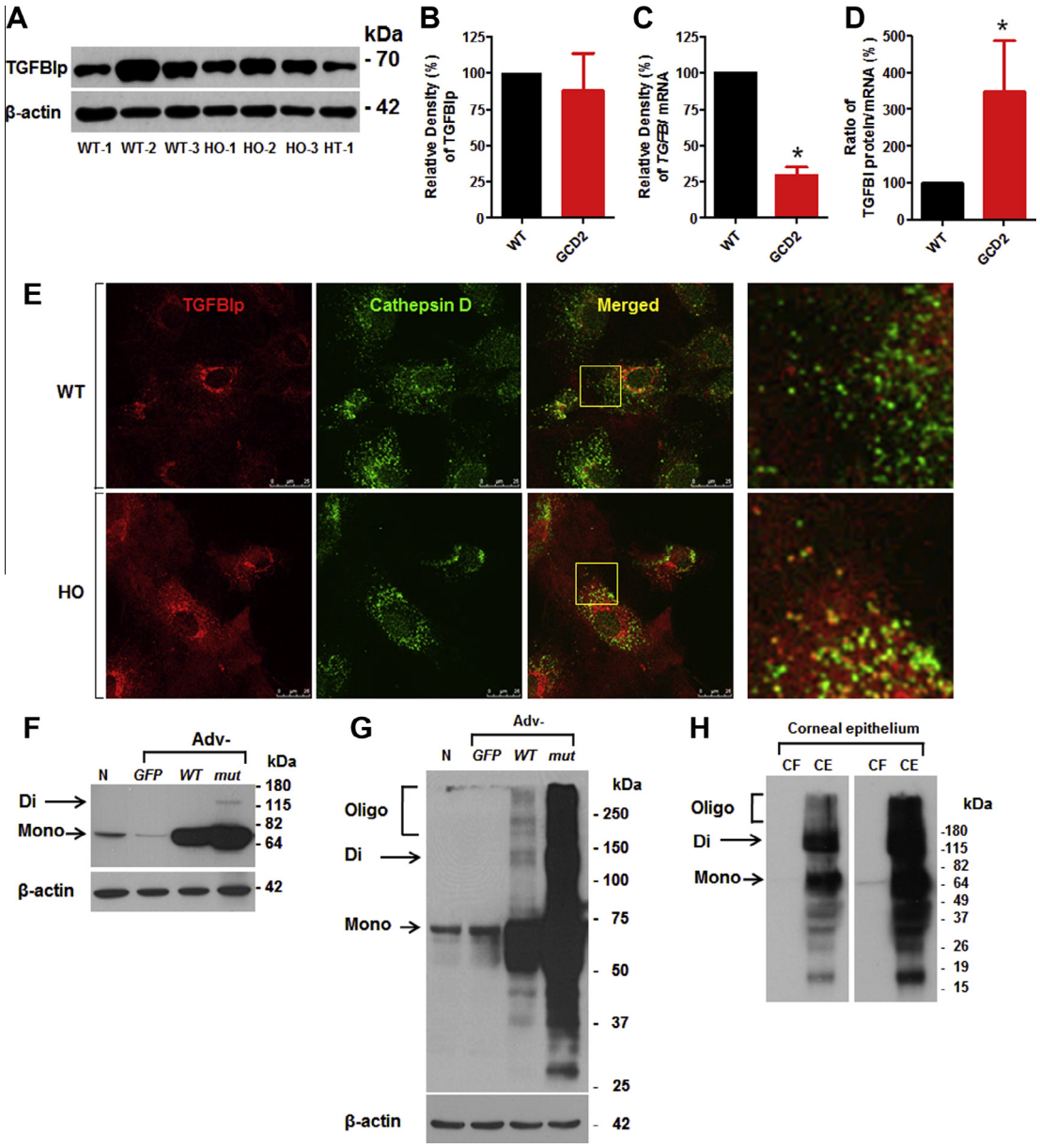

Fig. 1. Accumulated protein and decreased mRNA levels of *TGFBI* in GCD2 corneal fibroblasts. (A) TGFBIp expression as determined by Western blotting in three WT and four GCD2 corneal fibroblast samples. (B) Quantification of the TGFBI levels in (A). (C) *TGFBI* mRNA levels were determined using real-time PCR in WT and GCD2 corneal fibroblasts. *TGFBI* mRNA levels were significantly decreased in GCD2 compared with WT corneal fibroblasts. (D) TGFBIp levels in WT and GCD2 corneal fibroblasts were quantified by assessing the protein/mRNA ratio of *TGFBI*. Error bars represent the SDs of three independent experiments. $^{*}P < 0.05$. (E) Representative pictures of WT and HO corneal fibroblasts showing the localization of TGFBIp (red) and cathepsin D (green). (F) Adv-WT-TGFBIp and Adv-mutant-TGFBIp-infected cells were analyzed by Western blotting using an anti-TGFBIp antibody 48 h after infection. Dimer formation was detected only in mutant-TGFBIp cells (lane 4). (G) Six days later, dimers and oligomers in WT-TGFBIp and mutant-TGFBIp-infected cells were identified by Western blotting. (H) Patterns of TGFBIp in GCD2 HO patients. Dimerized or oligomerized TGFBIp was detected by Western blotting in corneal epithelia from GCD2 patients obtained during phototherapeutic keratectomy. The arrows and bracketed area indicate the position of the TGFBIp monomer (short arrows), putative dimer (long arrows), and putative oligomers (bracketed area). The right lane shows the molecular mass standards in kDa. N, not infected; CF, corneal fibroblast; CE, corneal epithelial deposits from GCD2 patients. (For interpretation of the references to color in this figure legend, the reader is referred to the web version of this article.)

HO corneal fibroblasts were stained with anti-TGFBIp and anti-cathepsin-D antibodies. Although both mutant- and WT-TGFBIp were found predominantly in the trans-Golgi network (TGN) (Fig. 1E), large amounts of TGFBIp were colocalized with cathepsin-D in HO cells. The accumulation of mutant-TGFBIp in lysosomal enzyme-containing vesicles suggests that mutant-TGFBIp is insufficiently degraded in GCD2 corneal fibroblasts.

We next examined the possibility that mutant-TGFBIp could accumulate in WT corneal fibroblasts by exogenously expressing mutant-TGFBIp. To overcome the low transfection efficiency in primary corneal fibroblasts, we used an adenovirus-mediated gene delivery system to express *TGFBI*. WT corneal fibroblasts were infected with adenovirus (Adv)-*TGFBI*, Adv-mutant-*TGFBI* fused to *GFP*, or control Adv. Corneal fibroblast cell extracts were examined by Western blotting with anti-TGFBIp antibody. Three days after infection, major immunoreactive bands were detected at ~70 kDa in cells infected with both Adv-*TGFBI* and Adv-mutant-*TGFBI* (Fig. 1F). Mutant-TGFBIp was also detected at ~140 kDa, corresponding to the dimeric form (Fig. 1F). Moreover, Western blotting in extracts harvested from mutant-*TGFBI* transfected cells

6 days after infection revealed increased levels of high molecular weight bands corresponding to dimeric and oligomeric TGFBIp, whereas only a faint band was observed in WT-TGFBI transfected cells (Fig. 1G). Because these results suggest the presence of dimeric and/or oligomeric mutant-TGFBIp in the corneal depositions of GCD2, we performed Western blotting under reducing conditions using corneal tissues isolated from a GCD2 HO patient under reducing conditions. Distinct bands of TGFBIp were observed over a broad range of sizes (Fig. 1H). The TGFBIp immunoreactive band patterns of WT corneal fibroblasts infected with Adv-mutant-*TGFBI* (Fig. 1G) were very similar to those from the cornea of a GCD2 HO patient (Fig. 1H).

3.2. Autophagy is activated in GCD2 corneal fibroblasts

To assess whether autophagy was induced to a greater extent by the intracellular accumulation of mutant-TGFBIp, we compared autophagy in WT and GCD2 corneal fibroblasts by using LC3 as a marker. Increased levels of LC3-II were detected in GCD2 corneal fibroblasts under normal culture, serum-free, and Earle's balanced salt solution (EBSS) conditions (Fig. 2A). In addition, to assess whether exogenous mutant-TGFBIp could induce autophagy in WT corneal fibroblasts, we measured LC3 in WT corneal fibroblasts infected with Adv-*TGFBI*, Adv-mutant-*TGFBI*, or control Adv-*GFP* using Western blotting. LC3-II levels were higher in WT fibroblasts infected with Adv-*GFP* and Adv-WT-*TGFBI* compared with non-infected cells. However, LC3-II levels were higher in WT corneal fibroblasts infected with Adv-mutant-TGFBIp compared with Adv-*TGFBI* (Fig. 2A and B). Because LC3-II levels correlate with the number of autophagosomes [21], increased LC3-II levels were consistent with an increased number of endogenous LC3-labeled puncta (Fig. 2C). Moreover, most endogenous LC3 colocalized with mutant-TGFBIp (Fig. 2C).

The increase in LC3-II levels and autophagosome numbers in GCD2 corneal fibroblasts is indicative of increased autophagy, and it could result from either increased autophagosome formation or decreased autophagosome degradation. To distinguish between these two possibilities, cells were treated with the lysosomal protease inhibitor leupeptin. If leupeptin did not increase LC3-II levels in GCD2 corneal fibroblasts relative to WT cells, then the increased LC3-II in GCD2 cells would be due reduced autophagic degradation, such as inhibited or delayed fusion between autophagosomes and lysosomes. However, treating GCD2 corneal fibroblasts with 5-μg/mL and 10-μg/mL leupeptin increased the levels of LC3-II by

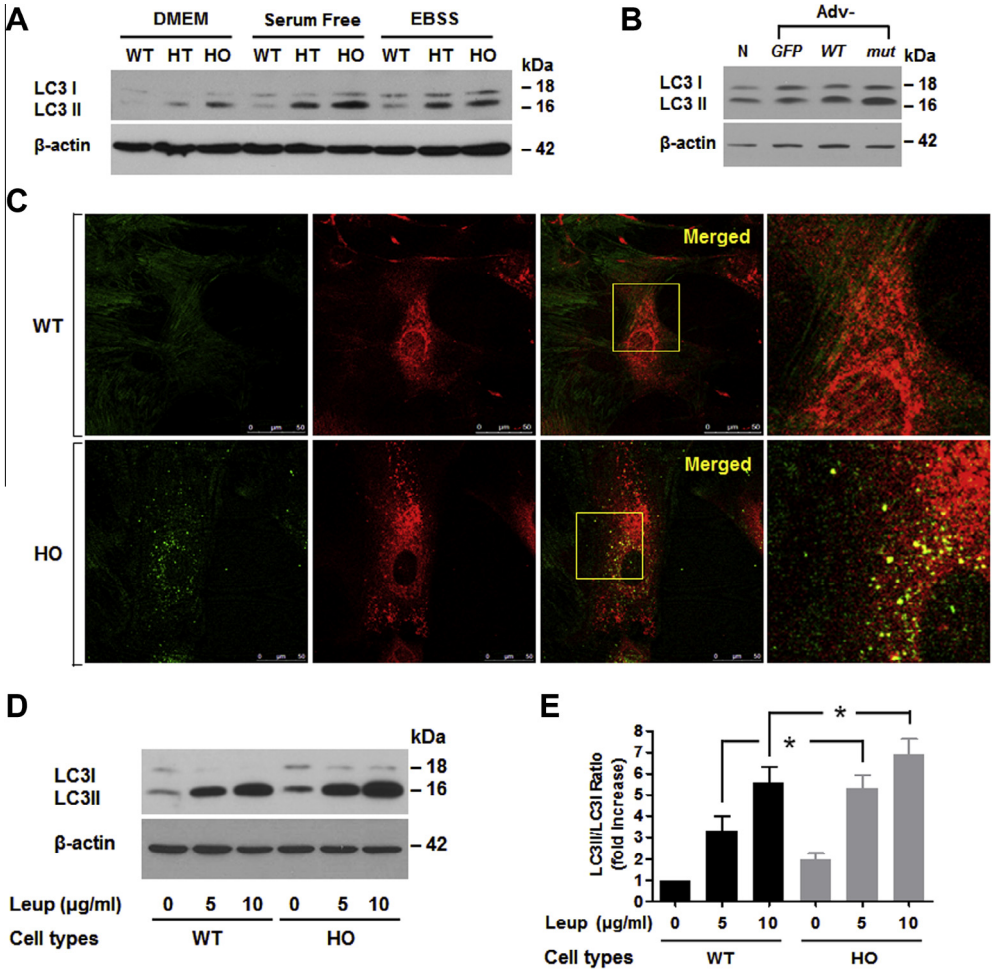

Fig. 2. Assessing autophagy induction in GCD2 corneal fibroblasts. (A) Representative analysis of the LC3-II by Western blotting using samples from wild type (WT), heterozygous (HT), and homozygous (HO) corneal fibroblasts in normal, serum-free and EBSS culture conditions. (B) Activation of autophagy in corneal fibroblasts overexpressing mutant-TGFBIp. (C) Representative images of WT and HO corneal fibroblasts expressing endogenous LC3. TGFBIp (WT or mutant)-expressing fibroblasts grown in complete media were fixed, permeabilized, and immunostained with antibodies against endogenous TGFBIp (red) and LC3 (green). LC3 exhibited vesicular staining; the number of LC3-positive puncta was higher in GCD2 HO corneal fibroblasts compared with control cells. Insets show a 3.5-fold magnification of the indicated region. A merged image of the red and green channels is shown in the third picture of each row; yellow indicates overlapping localization. (D) Leupeptin treatment significantly increased LC3-II levels in a dose-dependent manner in both WT and GCD2 HO corneal fibroblasts. (E) Densitometric analysis of the LC3-II/β-actin ratio using samples from wild-type (WT) and homozygous (HO) corneal fibroblasts in three independent experiments. Error bars represent the SDs of three independent experiments. $^{*}P < 0.05$. (For interpretation of the references to colour in this figure legend, the reader is referred to the web version of this article.)

5.326 ± 0.625-fold and 7.630 ± 0.703-fold, respectively ($P < 0.05$). In comparison, 3.831 ± 0.672-fold and 6.352 ± 0.741-fold increases were significantly observed in WT cells treated with 5 μg/mL and 10 μg/mL leupeptin, respectively ($P < 0.05$) (Fig. 2D and E). These results suggest that the increased LC3-II levels and autophagosome numbers could be due to the induction of autophagy.

3.3. Decreased levels of raptor induce autophagy in GCD2 corneal fibroblasts

To understand how mutant-TGFBIp induces autophagy, we next assessed whether the activation of autophagy in GCD2 corneal fibroblasts was mediated via mTOR. The levels of total and phosphorylated mTOR in WT corneal fibroblasts infected with Adv-mutant-TGFBIp were unchanged; however, raptor levels were decreased (Fig. 3A and D). Raptor was also expressed at significantly lower levels in GCD2 HO compared with WT primary corneal fibroblasts (Fig. 3B and E). GβL was not significantly expressed in WT corneal fibroblasts infected with Adv-mutant-TGFBIp (Fig. 3A and C). These data suggest that raptor might be downregulated in response to mutant-TGFBIp. In addition, the levels of p-P70S6K, the downstream substrate of mTOR, were reduced and was accompanied by an increase in LC3-II in WT corneal fibroblasts expressing reduced level of raptor after transfection with shRNA-raptor (Fig. 3F).

3.4. Selective degradation of raptor in mTORC1 through the UPS in GCD2 corneal fibroblasts

mTORC1 is known to be degraded via a UPS-dependent mechanism [22]. The findings of the present study indicate that the reduction in raptor levels in GCD2 corneal fibroblasts was most likely caused by proteolytic degradation rather than by the inhibition of transcription and/or translation. To confirm this, GCD2 HO corneal fibroblasts were pretreated with or without MG132, a specific inhibitor of the 26S proteasome. Without MG132 pretreatment, raptor levels were reduced in GCD2 corneal fibroblasts compared with WT corneal fibroblasts (Fig. 4A and B, lane 3). Interestingly, MG132 pretreatment inhibited the reduced raptor levels (Figs. 3A, lane 3 vs. lanes 4 and 5, and 4B).

Proteasome-mediated protein degradation signaling is generally initiated by the covalent attachment of multiple ubiquitin moieties to target proteins [23]. Therefore, we assessed the interaction between ubiquitin and raptor in WT and GCD2 corneal fibroblasts to investigate whether raptor is a UPS substrate. Corneal fibroblasts were treated for 12 h with or without MG132. Typical high molecular weight smeared bands of ubiquitin molecules were detected in both WT and GCD2 corneal fibroblasts treated with or without MG132 (Fig. 4C, lanes 1–4). Next, immunoprecipitations using anti-raptor antibodies were performed in the lysates of cells treated with or without MG132, followed by Western blotting for ubiquitin. More ubiquitinated raptor accumulated in MG132-treated cells (Fig. 4C, lanes 5 and 6 vs. lane 7 and 8). Furthermore, this degradation was blocked by pretreatment with MG132 (Fig. 4C, lane 8).

4. Discussion

The data described in the current study provide strong evidence that autophagy is induced in GCD2 corneal fibroblasts, but that its activation might be insufficient to facilitate the removal of mutant-TGFBIp. This leads to the pathological accumulation of autophagosomes and/or autophagolysosomes containing mutant-TGFBIp.

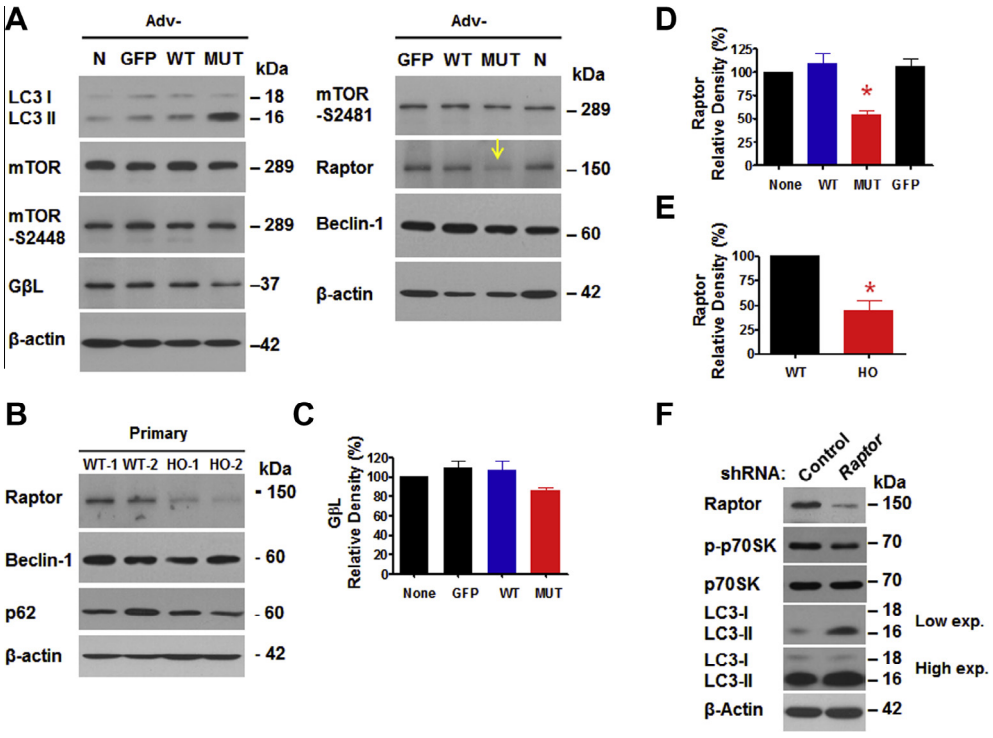

Fig. 3. Autophagy is induced by reduced raptor-dependent mTOR pathway in GCD2 corneal fibroblasts. Cell lysates prepared from WT corneal fibroblasts infected with Adv-*TGFBI*, Adv-mutant-*TGFBI*, or Adv-*GFP* were examined by Western blotting for the indicated proteins. (A) The expression of raptor was decreased in WT corneal fibroblasts infected with Adv-mutant-*TGFBI*. (B) The levels of raptor, beclin-1, and p62 were examined by Western blotting in primary cultured GCD2 HO and WT corneal fibroblasts. Expression of mutant-*TGFBI* decreased the levels of raptor, whereas beclin-1 and p62 were unchanged. (C) Quantification of the levels of GβL shown in (A). (D) Quantification of the levels of raptor shown in (A). (E) The expression of raptor decreased significantly in GCD2 HO corneal fibroblasts. (F) The p-P70S6K levels were reduced and was accompanied by an increase in LC3-II in WT corneal fibroblasts expressing reduced raptor after transfection with shRNA-raptor. Data are presented as the means ± SDs, $^{*}P < 0.05$. ↓ denotes slower migrating bands.

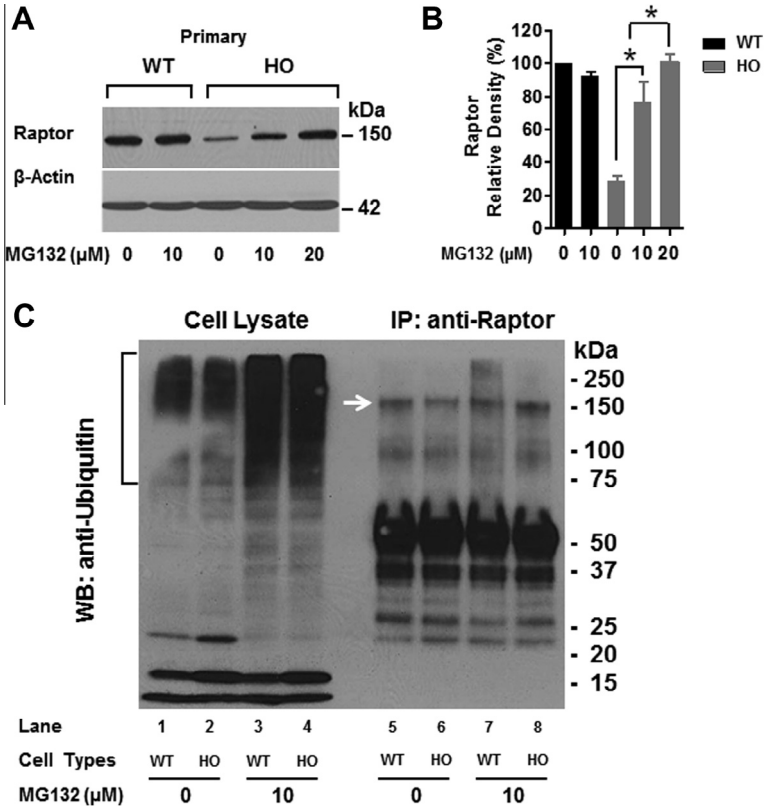

Fig. 4. Inhibiting proteasome activity increases the levels of endogenous raptor. (A) The proteasome inhibitor MG132 prevented raptor degradation and increased the levels of LC3-II in a dose-dependent manner. (B) Quantification of the raptor from (A). (C) Corneal fibroblasts were incubated in control medium or in the presence of MG132 for 12 h, and total cell lysates were immunoblotted with anti-ubiquitin antibodies. The bracket denotes higher molecular mass ubiquitinated products (lanes 1–4). Raptor was immunoprecipitated from cells, and the resulting immunoblots were probed with anti-ubiquitin antibodies (lanes 5–8). Arrow marks the position of bands from approximately 150 kDa to the ubiquitinated raptor. $^{*}P < 0.05$.

Mutant-TGFBIp accumulate in the autophagosomal and/or autophagolysosomal compartment of GCD2 corneal fibroblasts [18]. This could be explained by the increased expression of *TGFBI* gene in GCD2 corneal fibroblasts. In the present study, TGFBIp levels were not significantly different between WT and GCD2 HO corneal fibroblasts, which is consistent with the results of a previous study [24]. However, *TGFBI* mRNA levels were significantly lower in GCD2 HO corneal fibroblasts. This discrepancy suggests that mutant-TGFBIp is accumulated after defective degradation, rather than high gene expression. This is further supported by our observation that mutant-TGFBIp accumulates in corneal fibroblasts expressing exogenous mutant-*TGFBI*.

Autophagy is induced in GCD2 corneal fibroblasts, as confirmed by the following data. First, the basal levels of LC3-II were increased in GCD2 corneal fibroblasts and in a previously study [18], as well as in WT primary corneal fibroblasts overexpressing mutant-TGFBIp. Second, the number of endogenous LC3 puncta was significantly increased in GCD2 corneal fibroblasts; these puncta colocalized with mutant-TGFBIp [18]. Third, further accumulation of LC3-II occurred in GCD2 corneal fibroblasts in the presence of leupeptin. Fourth, increased levels of LC3-II were observed in GCD2 corneal fibroblasts compared with WT cells incubated in normal or serum-free media, and EBSS. Finally, the levels of raptor were significantly decreased in GCD2 corneal fibroblasts. Collectively, these data suggest that autophagy was induced but that its activation was insufficient to facilitate the removal of mutant-TGFBIp, leading to the pathological accumulation of autophagosomes and/or autophagolysosomes containing mutant-TGFBIp. This conclusion is supported by clearance of mutant-TGFBIp by activated autophagy (Supplementary data 1) and a previous study reporting that melatonin and rapamycin enhanced the elimination of mutant-TGFBIp by inducing autophagy in GCD2 fibroblasts [18,19]. Taken together, we can conclude that mutant-TGFBIp is insufficiently degraded by the autophagy–lysosome system in GCD2 corneal fibroblasts, even though they exhibit elevated basal levels of autophagy.

This study also demonstrated that, MG132 significantly prevented raptor reduction in GCD2 corneal fibroblasts, but that ubiquitinated raptor is increased in GCD2 compared with corneal fibroblasts. Once tagged with ubiquitin, substrate proteins are often targeted for rapid degradation in the UPS. Taken together, these data suggest that raptor could be rapidly degraded by the UPS during GCD2. Indeed, UPS should be activated in GCD2 corneal fibroblasts, which is supported by the accumulation of ubiquitinated proteins in GCD2 corneal fibroblasts [18]. Moreover, this UPS activation might play a protective role in GCD2 corneal fibroblasts because MG132 treatment significantly induced apoptotic cell death in a dose-dependent manner (Supplementary data 2). In addition, these data indicate that there is extensive crosstalk between the UPS and autophagy–lysosome systems, which were long considered independent degradation pathways with few or no points of interaction [25].

During the regulation of autophagy, reduced levels of raptor indicate that the activation of autophagy via mTOR pathway is related to the functional activity of the UPS. This notion is also supported by previous studies, where several key mTORC1 components such as mTOR, GβL, and raptor were degraded via the UPS following treatment with the anticancer agent perifosine [22]. However, in the present study, raptor was the only mTORC1 protein that was decreased in GCD2 corneal fibroblasts. Therefore,

further studies are required to understand the mechanism of selective raptor degradation associated with the ubiquitin–proteasome system.

In conclusion, the induction of high levels of autophagy could have beneficial effects in GCD2. It might enhance the removal of the toxic, disease-causing, and aggregation-prone mutant-TGFBIp protein, and might attenuate the cellular responses to various toxic insults. The results of this study suggest that an insufficient autophagy–lysosome pathway might be responsible for the intracellular accumulation of mutant-TGFBIp during the pathogenesis of GCD2.

Conflict of interest

The authors declare no conflict of interest.

Acknowledgments

The authors thank Jun-Young Oh, and Jun-Yup Jin for their technical assistance. This research was supported by a Basic Science Research Program through the National Research Foundation of Korea (NRF) funded by the Ministry of Education (NRF 2013R1A1A2012958), and by a National Research Foundation of Korea (NRF) grant funded by the Korean government (MEST) (2011-0028699).

Appendix A. Supplementary data

Supplementary data associated with this article can be found, in the online version, at http://dx.doi.org/10.1016/j.bbrc.2014.07.035.

References

[1] A. Ciechanover, Proteolysis: from the lysosome to ubiquitin and the proteasome, Nat. Rev. Mol. Cell Biol. 6 (2005) 79–87.
[2] S. Finkbeiner, A.M. Cuervo, R.I. Morimoto, P.J. Muchowski, Disease-modifying pathways in neurodegeneration, J. Neurosci. 26 (2006) 10349–10357.
[3] T. Lamark, T. Johansen, Autophagy: links with the proteasome, Curr. Opin. Cell Biol. 22 (2010) 192–198.
[4] Y. Ohsumi, Molecular dissection of autophagy: two ubiquitin-like systems, Nat. Rev. Mol. Cell Biol. 2 (2001) 211–216.
[5] T. Yorimitsu, D.J. Klionsky, Autophagy: molecular machinery for self-eating, Cell Death Differ. 12 (Suppl. 2) (2005) 1542–1552.
[6] A.M. Cuervo, Autophagy: many paths to the same end, Mol. Cell Biochem. 263 (2004) 55–72.
[7] K. Hara, Y. Maruki, X. Long, K. Yoshino, N. Oshiro, S. Hidayat, C. Tokunaga, J. Avruch, K. Yonezawa, Raptor, a binding partner of target of rapamycin (TOR), mediates TOR action, Cell 110 (2002) 177–189.
[8] D.H. Kim, D.D. Sarbassov, S.M. Ali, R.R. Latek, K.V. Guntur, H. Erdjument-Bromage, P. Tempst, D.M. Sabatini, GbetaL, a positive regulator of the rapamycin-sensitive pathway required for the nutrient-sensitive interaction between raptor and mTOR, Mol. Cell 11 (2003) 895–904.
[9] D.D. Sarbassov, S.M. Ali, D.M. Sabatini, Growing roles for the mTOR pathway, Curr. Opin. Cell Biol. 17 (2005) 596–603.
[10] R. Loewith, E. Jacinto, S. Wullschleger, A. Lorberg, J.L. Crespo, D. Bonenfant, W. Oppliger, P. Jenoe, M.N. Hall, Two TOR complexes, only one of which is rapamycin sensitive, have distinct roles in cell growth control, Mol. Cell 10 (2002) 457–468.
[11] T. Noda, Y. Ohsumi, Tor, a phosphatidylinositol kinase homologue, controls autophagy in yeast, J. Biol. Chem. 273 (1998) 3963–3966.
[12] A.J. Meijer, P. Codogno, Signalling and autophagy regulation in health, aging and disease, Mol. Aspects Med. 27 (2006) 411–425.
[13] J. Skonier, M. Neubauer, L. Madisen, K. Bennett, G.D. Plowman, A.F. Purchio, CDNA cloning and sequence analysis of beta ig-h3, a novel gene induced in a human adenocarcinoma cell line after treatment with transforming growth factor-beta, DNA Cell Biol. 11 (1992) 511–522.
[14] G.K. Klintworth, Advances in the molecular genetics of corneal dystrophies, Am. J. Ophthalmol. 128 (1999) 747–754.
[15] E. Korvatska, H. Henry, Y. Mashima, M. Yamada, C. Bachmann, F.L. Munier, D.F. Schorderet, Amyloid and non-amyloid forms of 5q31-linked corneal dystrophy resulting from kerato-epithelin mutations at Arg-124 are associated with abnormal turnover of the protein, J. Biol. Chem. 275 (2000) 11465–11469.
[16] S.I. Choi, T.I. Kim, K.S. Kim, B.Y. Kim, S.Y. Ahn, H.J. Cho, H.K. Lee, H.S. Cho, E.K. Kim, Decreased catalase expression and increased susceptibility to oxidative stress in primary cultured corneal fibroblasts from patients with granular corneal dystrophy type II, Am. J. Pathol. 175 (2009) 248–261.
[17] T.I. Kim, H. Kim, D.J. Lee, S.I. Choi, S.W. Kang, E.K. Kim, Altered mitochondrial function in type 2 granular corneal dystrophy, Am. J. Pathol. 179 (2011) 684–692.
[18] S.I. Choi, B.Y. Kim, S. Dadakhujaev, J.Y. Oh, T.I. Kim, J.Y. Kim, E.K. Kim, Impaired autophagy and delayed autophagic clearance of transforming growth factor beta-induced protein (TGFBI) in granular corneal dystrophy type 2, Autophagy 8 (2012) 1782–1797.
[19] S.I. Choi, K.S. Kim, J.Y. Oh, J.Y. Jin, G.H. Lee, E.K. Kim, Melatonin induces autophagy via an mTOR-dependent pathway and enhances clearance of mutant-TGFBIp, J. Pineal Res. 54 (2013) 361–372.
[20] J. Luo, Z.L. Deng, X. Luo, N. Tang, W.X. Song, J. Chen, K.A. Sharff, H.H. Luu, R.C. Haydon, K.W. Kinzler, B. Vogelstein, T.C. He, A protocol for rapid generation of recombinant adenoviruses using the AdEasy system, Nat. Protoc. 2 (2007) 1236–1247.
[21] Y. Kabeya, N. Mizushima, T. Ueno, A. Yamamoto, T. Kirisako, T. Noda, E. Kominami, Y. Ohsumi, T. Yoshimori, LC3, a mammalian homologue of yeast Apg8p, is localized in autophagosome membranes after processing, EMBO J. 19 (2000) 5720–5728.
[22] L. Fu, Y.A. Kim, X. Wang, X. Wu, P. Yue, S. Lonial, F.R. Khuri, S.Y. Sun, Perifosine inhibits mammalian target of rapamycin signaling through facilitating degradation of major components in the mTOR axis and induces autophagy, Cancer Res. 69 (2009) 8967–8976.
[23] A. Hershko, A. Ciechanover, The ubiquitin system, Annu. Rev. Biochem. 67 (1998) 425–479.
[24] K.E. Han, S.I. Choi, W.S. Chung, S.H. Jung, N. Katsanis, T.I. Kim, E.K. Kim, Extremely varied phenotypes in granular corneal dystrophy type 2 heterozygotes, Mol. Vis. 18 (2012) 1755–1762.
[25] A. Lilienbaum, Relationship between the proteasomal system and autophagy, Int. J. Biochem. Mol. Biol. 4 (2013) 1–26.